Article:
Suarez-Jimenez, Benjamin, Bisby, James A, Horner, Aidan James orcid.org/0000-0003-0882-9756 et al. (3 more authors) (2018) Linked networks for learning and expressing location-specific threat. Proceedings of the National Academy of Sciences of the United States of America. E1032-E1040. ISSN 1091-6490

https://doi.org/10.1073/pnas.1714691115

Linked networks for learning and expressing location-specific threat

*Benjamin Suarez-Jimenez[† 1,4], James A. Bisby[† 1,2], Aidan J. Horner[3], John A. King[5], Daniel S. Pine[4], *Neil Burgess[1,2]

[†]These authors contributed equally to this work

[1]*Institute of Cognitive Neuroscience, University College London*

[2]*Institute of Neurology, University College London*

[3]*Department of Psychology, University of York*

[4]*Section of Developmental Affective Neuroscience, National Institute of Mental Health*

[5]*Department of Clinical Psychology, University College London*

***Authors for correspondence:**
Benjamin Suarez-Jimenez & Neil Burgess
UCL Institute of Cognitive Neuroscience, London, WC1N 3AR, UK
Email: benjamin.jimenez@nih.gov, n.burgess@ucl.ac.uk
Tel: +44 20 7679 1147; Fax: +44 20 7813 2835

Category: Biological Sciences - Neuroscience
Keyword: fMRI, location-specific threat conditioning, hippocampus, navigation, learning

Abstract

Learning locations of danger within our environment is a vital adaptive ability whose neural bases are only partially understood. We examined fMRI brain activity while participants navigated a virtual environment which flowers appeared and were "picked." Picking flowers in the danger zone (half of the environment) predicted an electric shock to the wrist (or "bee-sting"); flowers in the safe zone never predicted shock; and household objects served as controls for neutral spatial memory. Participants demonstrated learning with shock expectancy ratings and skin conductance increases for flowers in the danger zone. Patterns of brain activity shifted between overlapping networks during different task stages. Learning about environmental threats, during flower approach in either zone, engaged the anterior hippocampus, amygdala, and vmPFC, with vmPFC-hippocampal functional connectivity increasing with experience. Threat appraisal, during approach in the danger zone, engaged the insula and dorsal anterior cingulate (dACC), with insula-hippocampal functional connectivity. During imminent threat, after picking a flower, this pattern was supplemented by activity in periaqueductal gray (PAG), insula-dACC coupling, and posterior hippocampal activity that increased with experience. We interpret these patterns in terms of multiple representations, of: spatial context (anterior hippocampus); specific locations (posterior hippocampus); stimuli (amygdala); value (vmPFC); threat – both visceral (insula) and cognitive (dACC); and defensive behaviors (PAG), interacting in different combinations to perform the functions required at each task stage. Our findings illuminate how we learn about location-specific threats and suggest how they might break-down into overgeneralization or hypervigilance in anxiety disorders.

Significance statement

When exploring our world, we must learn about the identity and location of threats. Despite the adaptive significance of these processes, little is known about the component processes, which allow human learning. We delineate these processes engaged as people learn associations between spatial location and its aversive value in a virtual environment. vmPFC, anterior hippocampus and amygdala form a network that supports such learning. dACC and insula engagement reflect the cognitive and visceral appraisal of looming danger. Encounters with imminent threats recruit the periaqueductal grey with the initiation of defensive behavior. Findings highlight how networks of distributed brain structures interact to support distinct processes engaged during learning, each of which may malfunction to give risk to features of psychological disorders.

Learning the locations of threats is essential for survival, and impairment in this ability generates debilitating symptoms of anxiety disorders, such as avoidance and over-generalization of fear (1–3). Previous work has shown how discrete threat-related cues or contexts impact behavior (4–7), and research in rodents has distinguished the brain areas supporting particular features of threat-related learning (8–13). In addition, several neuroimaging studies identify brain regions engaged when people learn to associate threat with discrete stimuli and contexts. However, most research in humans relies on static images and simple paradigms that fail to capture key aspects of the scenarios which generate fear in patients. As such, relatively little research maps the way in which networks of brain regions interact to support clinically-relevant behaviors. Avoidance of dangers that are specific to one area of an environment without impacting on behavior in other (safe) areas represents one such clinically-relevant behavior that can be modeled using virtual reality and the techniques of systems neuroscience. Accordingly, we developed a novel, naturalistic paradigm in which to study learning of the environmental location of a specific threat and its expression in behavior.

When exploring an environment, the hippocampus is thought to store spatial representations of the surrounding context and embedded locations (14–16). The binding of these representations allows organisms to learn about threat, with the hippocampus crucial for modulating the context-dependence of fear and its extinction (8, 13, 17, 18). Studies in rodents distinguish functions of the dorsal hippocampus, which stores contextual representations, from the ventral hippocampus, which may mediate anxiety-like behavior (19–21, 21, 22), a difference potentially reflected in the size of place fields along the dorsoventral axis (22–24).

In humans, a similar dissociation along the posterior-anterior axis of the hippocampus has been proposed, corresponding to the dorsoventral axis in rodents (21, 25–27). For example, activity in the posterior hippocampus has been shown to correlate with spatial memory for object locations within a virtual environment, whilst activity in the anterior hippocampus correlates with novelty (28, 29). Further, the anterior hippocampus appears to be involved in processing environmental threat, with greater activity corresponding to increasing levels of threat, whether triggered by the presence of a sleeping predator (30) or a prior association between a virtual context and electric shock (17).

During threat, the dorsal anterior cingulate cortex (dACC) and dorsomedial prefrontal cortex are involved in the appraisal and expression of conditioned responses (31–33). By contrast, the ventromedial prefrontal cortex (vmPFC) is a primary candidate for providing top-down regulation

of fear and anxiety (34–39); vmPFC shows synchronized activity with the anterior hippocampus as rodents approach dangerous parts of an environment (40, 41). The vmPFC is more generally associated with value-based decision making (42–44) which would include assessment of environmental threat. Thus, the anterior hippocampus and both dorsal and ventral mPFC may interact to support behavior in response to environmental threat (45–47).

As a threat becomes imminent, defense reactions are triggered, often involving active escape or avoidance (48–50). Engagement of immediate survival actions is thought to be supported by the amygdala and midbrain structures, including the periaqueductal gray (10, 51). The amygdala also allows organisms to associate discrete cues with aversive properties (10, 52–54) and is thought to interact with the PAG to process information about the unconditioned stimulus (55) and initiate defense behaviors (56). In humans, imminent threat increases overall activity in the PAG and its functional coupling with dACC (57, 58) to support fear expression.

Here we used a virtual environment and functional magnetic resonance imaging (fMRI) to extend past work. Specifically, we capture the behavior and patterns of brain activity as people are learning the environmental locations of dangers, and as they are approaching locations associated with danger or safety. The virtual environment consisted of a walled arena with distant cues for orientation and identical cues (flowers) whose association with threat depended only on their location within the environment. Participants navigated in this environment and alternatively completed one of two tasks: (1) picking flowers that might contain a bee, as indicated by a mild electric shock representing a sting (shocks were restricted to one-half of the environment); or (2) collecting objects, and later replacing them to test memory for their location. This task allowed us to differentiate neural responses associated with various aspects of learning in both dangerous and safe parts of a single environment. Previous literature suggests hippocampal and mPFC involvement in learning and appraisal of environmental threat, and amygdala and midbrain involvement in fear expression. Here we hoped to identify the sequences of activity in these and related regions, and patterns of functional connectivity between them, as a location becomes associated with threat and during the approach to such a location.

Results

Behavioral and Skin Conductance Results

As participants explored the virtual environment (**Fig. 1A and B**; see Methods for further details), they were required to navigate towards flowers that appeared one at a time in different locations. As a flower was touched (picked), they were held stationary for a variable duration (2-8 seconds) and required to rate their expectancy for receiving a shock/sting (rating of 0-9). Flowers located in one-half of the environment were paired with shock (danger zone; delivered at the end of the stationary period on 50% of trials), whereas flowers in the other half of the environment were never paired with shock (safe zone). All flowers were the same and their predictive value (danger or safety) could not be distinguished by visual appearance alone.

We first compared skin conductance level (SCL; tonic changes in skin conductance) during periods when participants approached flowers. During these periods, we compared SCL between flowers located in dangerous and safe areas of the environment (mean duration of approach periods = 8.95 sec ±2.27); we also assessed changes in SCL from early to late stages of the experiment (collapsing trials into four blocks; 10 trials in each block). A 2x4 ANOVA (zone x block) showed greater SCL when approaching flowers located in dangerous relative to safe areas (**Fig. 1C**; $F(1,21)=8.92$, $p<0.01$; no main effect of block, $F(3,63)=1.01$, $p>0.05$, or zone x block interaction, $F(3,63)=1.37$, $p>0.05$).

We next examined skin conductance responses (SCR) immediately after participants touched the flower, during the stationary period (mean duration = 5.02 sec ±0.44 sec). A 2x4 ANOVA (zone x block) revealed greater SCRs to flowers located in dangerous compared to safe zones (**Fig. 1D**; $F(1,21)=7.76$, $p<0.01$). We also saw a significant effect of block ($F(3,63)=16.06$, $p<0.01$; no zone x block interaction, $F(3,63)=1.69$, $p>0.05$) reflecting a general decrease in SCRs as the experiment progressed (block 1 v block 4, $t(21)=4.88$, $p<0.001$).

Assessing shock expectancy ratings (**Fig. 1E**), a 2x4 ANOVA (zone x block) showed a significant zone x block interaction ($F(3,63)=20.76$, $p<0.01$) and significant main effects of block ($F(3,63)=9.98$, $p<0.01$) and zone ($F(1,21)=135.55$, $p<0.01$). Further analysis of the interaction showed that, whilst shock expectancy ratings to flowers associated with danger increased from block 1 to block 4 ($t(21)=3.08$, $p<0.01$), they decreased for flowers predicting safety (block 1 v block 4, $t(21)=6.50$, $p<0.001$). Indeed, this pattern was confirmed with a greater increase in shock expectancy during block 4 for flowers associated with danger relative to safety (danger minus safety) compared to block 1 ($t(21)=6.32$, $p<0.001$). In summary, participants were quick to learn the contingencies between flowers and their location within the environment. We saw greater skin conductance during approach and stationary periods for flowers located in the environment

associated with shock. Also, shock expectancy ratings showed a similar pattern with higher ratings for flowers predicting danger.

Interleaved with these flower trials, participants performed a spatial memory task within the same environment (see Methods for further details). Participants were required to learn the location of four objects, with two objects appearing in each side of the environment (i.e., the safe or danger zones, although objects were never paired with shock). Participants were required to replace objects where they had been found, and distance error from the correct location provided a measure of performance. Like threat analyses, trials were partitioned into four equal blocks. A 2x4 within-subjects ANOVA (zone x block) on mean object placement distance error showed a significant effect of block ($F(3,63)=14.98$, $p<0.01$; no main effect of zone or zone x block interaction, $F's<1$). A direct comparison of performance across test blocks showed that distance error decreased from block 1 to block 4 ($t(21)=6.00$, $p<0.01$; **Fig. S1**) reflecting improved spatial memory performance irrespective of whether objects had been located in the danger or safe zones of the flower task.

fMRI Results

Approach periods: Differences between learning about threat and object locations

We first mapped areas that were differentially involved in performing the two tasks, contrasting brain activity as participants approached flowers (collapsing across danger and safe conditions) with object approach periods when participants were instructed to collect the object and remember their spatial location (i.e. omitting object replacement trials; mean duration of approach = 14.91 sec ±6.89 sec). Each period began at trial onset, either when the next flower or next object appeared in the environment, and each period ended when that flower or object was "collected." We then analyzed the final 75% of the approach period, omitting the initial 25% to remove orienting behavior preceding active navigation. To assess differences in learning across the two tasks, we divided trials into blocks comprising the first- (early) and last-half (late) of the experiment, and whether approaching a flower or object, resulting in a 2x2 ANOVA with factors of task (object or flower) and block (early, late; see Table S1 for full results from this analysis).

When approaching flowers during threat learning (flowers > objects), we saw greater activity in a range of regions often associated with fear learning and memory, including vmPFC, dACC, anterior hippocampus, amygdala ($p<0.05$ FWE SVC; **Fig. 2A upper panel**), posterior cingulate

cortex (PCC), medial parietal cortex and insula ($p<0.05$ FWE; medial parietal activity extending into precuneus and retrosplenial cortex at $p<0.001$ uncorrected). When approaching objects (objects > flowers), a different network of areas showed greater activity including the left middle frontal gyrus, middle temporal gyrus, inferior parietal lobule and inferior frontal gyrus, right precentral gyrus, inferior frontal gyrus and an area extending across lingual and parahippocampal gyri ($p<0.05$ FWE; **Fig. 2A lower panel**). These results highlight two distinct networks recruited when learning about environmental threat or general spatial memory for object locations (there was no effect of block when contrasting early versus late blocks).

Interestingly, we saw a task by block interaction in the hippocampus, amygdala ($p<0.05$ FWE SVC; **Fig. 2B left panel**), and vmPFC and medial parietal areas (including precuneus, and PCC; $p<0.05$ FWE; extending to the retrosplenial cortex at $p<0.001$ uncorrected; **Fig. 2B right panel**). Activity in these areas was greater when approaching flowers compared to objects and this difference was greater during the last half compared to the first half of the experiment. In summary, although several higher cortical areas showed more activity when approaching objects in the spatial memory task, mPFC, anterior hippocampus, and amygdala demonstrated greater activity when approaching flowers during threat learning, an effect that increased from the first to last half of the experiment.

Approach periods: Differences between flowers predicting danger or safety

We compared brain activity as individuals approached flowers located in the danger and safe zones of the environment. We again divided trials into two blocks comprising the first- (early) and last-half (late) of the experiment producing a 2x2 ANOVA with factors of zone (danger, safety) and block (early, late; see Table S2 for full results from this analysis). When approaching flowers located in the danger zone (danger > safe), we saw greater activity in dACC ($p<0.05$ FWE SVC; **Fig. 3A**) and bilateral insula ($p<0.001$ uncorrected). The reverse contrast (safe > danger) revealed no significant effects even when using a lenient threshold ($p<0.001$ uncorrected).

Next, we looked for brain areas that showed greater activity during the second half of the experiment compared to the first half (late > early), reflecting changes over time as participants learned about the environment, irrespective of which zone they were in. This analysis showed greater activity during the second half of the experiment in medial parietal areas (including precuneus, retrosplenial cortex, and PCC), vmPFC and the right hippocampus ($p<0.05$ FWE; greater activity was also seen in the left hippocampus using small volume correction, $p<0.05$ FWE

SVC; **Fig. 3B**). The reverse contrast, identifying areas more active during the first half of the experiment (early > late), showed greater activity in the right insula and ventrolateral PFC ($p<0.05$ FWE). There was no zone (safe, danger) by block (early, late) interaction during the approach periods to flowers, possibly due to the rapid learning of contingencies as indicated by our SCR results.

Given our hypothesis that the hippocampus represents the spatial context, to which participants learned to associate danger, we next looked for brain activity when approaching flowers correlated over trials with hippocampal activity as a function of either zone (danger, safety) or block (early, late). We, therefore, performed two separate psychophysiological interaction analyses (59) on data from approach periods, using the right hippocampus as a seed region (MNI coordinates: 27, -18, -15; defined from our late versus early approach contrast). Results revealed a positive correlation between the hippocampus and bilateral insula ($p<0.001$ uncorrected) when approaching flowers located in part of the environment associated with danger compared to safety and between the hippocampus and vmPFC ($p<0.001$ uncorrected) during the last half of learning compared to the first-half.

In summary, vmPFC and hippocampus showed increased activity during approach periods as learning progressed and showed increased functional connectivity during the task. These results suggest the involvement of the vmPFC and hippocampus in learning about the context, although changes in activity did not discriminate between danger and safety. On the other hand, dACC activity and coupling between the right hippocampus and insula increased when approaching flowers in the dangerous compared to safe zone throughout the whole task.

Stationary Periods: Differences between flowers predicting danger and safety

We next examined brain activity when participants were held stationary after picking flowers and anticipating a potential shock, comparing across danger and safe zones and early and late halves of the experiment. During these stationary periods, flowers located in an area of the environment associated with danger (danger > safety) generated greater activity in the caudate, dACC, bilateral insula and an area of the midbrain, including the periaqueductal gray ($p<0.05$ FWE; **Fig. 4A**). For the reverse contrast, flowers located in the safe zone of the environment (safety > danger) were associated with greater activity in vmPFC although at a more liberal threshold ($p<0.001$ uncorrected; **Fig. 4A**), consistent with an estimation of value.

We found an effect of block with increased activity during the last-half of learning (late > early) in bilateral posterior hippocampus ($p<0.05$ FWE SVC; **Fig. 4B**). We saw no significant changes in activity for the reverse contrast (early > late) nor any interaction effects between zone (safe, danger) and block (early, late), again possibly reflecting the rapid learning of contingencies as observed in our SCR result.

Given that activity in dACC was greater during stationary periods when located in areas of the environment predicting danger, we next looked whether this area showed increased functional correlations with other brain regions as a function of threat (danger > safety). A PPI analysis using dACC as a seed region (defined from our danger > safety contrast during stationary periods) showed increased functional connectivity with bilateral insula in danger compared to safe zones ($p<0.001$ uncorrected).

In summary, areas often involved in imminent threat including dACC, insula, PAG and caudate showed greater activity during stationary periods after picking flowers in parts of the environment associated with danger. Greater functional connectivity between the dACC and insula was also seen during stationary periods for flowers located in the danger zone. In contrast, vmPFC showed greater activity during stationary periods when picking flowers in areas associated with safety throughout the whole experiment.

Discussion

We examined how people learn to recognize features of dangerous objects while mapping the brain networks that support components of such learning. Our task was designed in such a way that participants had to rely on spatial memory to learn threat contingencies and could not discriminate danger and safety based on the visual properties of flowers alone, a process likely supported by amygdala-dependent reinforcement learning (53, 54, 60). We demonstrated physiological and subjective signatures of location-specific threat as evidenced by greater skin conductance responses and shock expectancy ratings for flowers located in the danger zone. Learning about environmental threat, when approaching flowers in either zone, was associated with greater activity in the anterior hippocampus, vmPFC, and amygdala, with vmPFC-hippocampal functional connectivity increasing with experience (see **Fig. 5A**). During the appraisal of threat as flowers located in the danger zone were approached, we saw increased activity in the insula and dACC, along with greater insula-hippocampal functional connectivity (see **Fig. 5B**). During imminent threat, after picking a flower, this pattern was extended with activity in

PAG and insula-dACC coupling (see **Fig. 5C**). Further, we saw a dissociation along the long axis of the hippocampus with greater posterior activity during imminent threat as opposed to anterior hippocampal activity during approach. In contrast, a network of areas in frontal, parietal, and temporal lobes was observed during spatial memory for unemotional objects. Our results highlight distinct networks that appear crucial in the successful provision of multiple representations to facilitate learning, appraisal, and behavioral responses to environmental threat.

Learning about danger within an environment requires the integration of location information with acquired value-based contingencies, processes thought to involve synchronization of neural activity in rodent homologs of anterior hippocampus and vmPFC (7, 40, 61). Our results suggest that similar anterior hippocampus-vmPFC communication might support analogous forms of learning in humans. While activity in vmPFC and anterior hippocampus did not differentiate danger and safety when approaching flowers, it increased with experience (from first- to last-half of the experiment), as did functional connectivity between them. This hippocampus-vmPFC engagement suggests a role in learning about environmental locations that is potentiated by the threat-related flower task compared to the spatial memory task (approaching objects). This would be consistent with findings that vmPFC involvement in memory increases with the subjective salience or value of the memoranda (e.g. (62, 63). Thus vmPFC may integrate evaluative processes with a hippocampal provision of spatial location to establish the distribution of environmental threat.

Other key memory-related areas also showed increased activity in late compared to early blocks only when approaching flowers, not when approaching objects, including retrosplenial cortex and precuneus. Again, activity in these areas may be specifically involved in threat learning discrimination (64, 65). However, it is also possible that increased activity in these anterior and posterior midline regions reflects encoding of the broader, less precise, location associated with threat compared to the specific locations of objects in the spatial memory tasks.

Furthermore, approaching flowers that predicted danger (compared to those in the safe zone) was associated with greater activity in dACC and insula, two regions often co-active during emotional processing (66). When approaching danger, the insula might provide interoceptive signals of anxiety and fear (67) to be integrated with cognitive-based appraisal in dACC (68, 69). As activity in regions distinguishing danger and safety did not alter over time (i.e., no zone x block interaction), we assume that internal affective representations were acquired rapidly within our task, as indicated by the fast separation of skin conductance levels and shock expectancy ratings

between danger and safety. Further, increased insula-anterior hippocampus connectivity when approaching flowers associated with danger suggests that the hippocampus might relay location information to support internal signals of threat.

We saw a clear dissociation within the hippocampus, consistent with prior work in rodents. Specifically, we observed greater activity during the second as compared to the first half of the experiment in the anterior hippocampus during approach; this contrasts with activity in the posterior hippocampus, which was elevated after picking flowers, regardless of their location. This hippocampal dissociation might relate to the increasing size of place fields from the rodent homologs of posterior to anterior hippocampus (70). Thus, the anterior hippocampus might allow the more distributed potential threat (any flowers in the danger zone) to be associated with a broader spatial context. In contrast, the posterior hippocampus could support the more precise association of threat to the specific location of the shock when delivered. Such an interpretation would be consistent with the posterior medial temporal activity observed in the spatial memory task, in which the specific locations of individual objects had to be remembered.

Our anterior hippocampal effect during approach was more posterior than in other human studies using anxiogenic tasks (17, 30), possibly due to subtle differences in experimental design. In previous studies, an aversive shock was predicted by an approaching predator (30), or while passively watching a video clip of a virtual environment (17), so that danger was not so clearly restricted by the spatial location within the overall context. In our task, danger was restricted to half of the environment and location (in or out of the danger zone) was always important for prediction. We speculate that when coarser conceptual representations of space and broader contexts can be used to inform behavior, hippocampal activity will be more anterior reflecting larger place fields (27, 70, 71).

Imminent threat during stationary periods in the danger zone was characterized by greater activity in insula and dACC and increased functional connectivity between them. Activity in these areas, seen during both approach and stationary periods, likely reflects integration of visceral feelings and cognitive appraisals of threat to trigger threat detection and fear expression (58). Imminent threat was also associated with increased PAG activity, an area known to drive immediate defense reactions (72–74), and thought to receive inputs from dACC and insula to promote behavioral responses to threat (75). This network of areas might work in concert to produce anxiety and fear to guide defensive behavior, with the PAG implicated in flight and immobility responses in rodents (56, 74, 76) and feelings of dread for a looming shock in humans (58).

Consistent with proposed dissociable roles for mPFC subregions during fear learning (31, 77), while dACC activity was greater for flowers predicting danger, greater vmPFC activity during stationary periods was observed for flowers predicting safety, albeit at a more liberal threshold. The vmPFC has been implicated in tracking positively valued options (44) and supporting inhibition of previously learned fear responses (32, 34), with dorsal and ventral sub-regions of vmPFC proposed to support such value representation and inhibition of learned responses, respectively (78). Typically ypically, studies show vmPFC recruitment after initial fear has been acquired and then extinguished (32, 34, 61) or when fear and safety signals are reversed (37), also supporting a role in inhibition. It is plausible that individuals initially learn more generalized fear representations across an environment and, as more specific location information is acquired, via functional connectivity with hippocampus, behavioral responses are refined by vmPFC-mediated inhibition of fear responses falling outside of the appropriate locations (18, 35, 45). Overall, we show a clear dissociation between areas of mPFC (i.e. dACC and vmPFC) that work to promote or inhibit behavioral responses (36, 38).

Our findings have clear clinical implications for learning about environmental threat and its later expression. Abnormal responding of the hippocampus, insula, and dACC has been noted in patients suffering from anxiety disorders (79, 80), possibly contributing to generalized anxiety and fear across environmental stimuli. Context plays an important role in fear conditioning, informing an individual whether stimuli predict safety or danger. It is important to distinguish between the relatively well studied mechanisms, focusing on the amygdala, associating fearful responding to specific objects (9, 10) from the mechanisms of contextual-modulation of these fearful responses. In some psychopathologies, it is specifically the discrimination between safety and danger contexts that is impaired, with dysfunction of both hippocampus and mPFC implicated (1, 81). These patients often show an overgeneralization of, or an exaggerated response to, threat into contexts predicting safety (74).

Here we found that activity in the anterior hippocampus, mPFC, and insula reflects experience of the distribution of danger within a single environment. The functional connectivity between anterior hippocampus and mPFC increases as the task is learned, suggesting that hippocampal inputs to mPFC allow the inhibition of contextually inappropriate responses to fear. In addition, functional connectivity between anterior hippocampus and insula increased in dangerous compared to safe locations, suggesting a hippocampal contribution to context-specific interoceptive sensations of dread. As such, our results indicate disrupted communication with anterior hippocampus as a key factor in some aspects of hypervigilance and over-generalization

of fear within anxiety disorders and PTSD. To test this hypothesis, future studies should target anterior hippocampal communication with insula and mPFC in clinical populations performing naturalistic virtual context conditioning tasks. Such experiments could establish whether fMRI (or MEG; (29, 82–85) correlates of inter-regional communication relate to specific sets of symptoms such as hypervigilance, avoidance, or exaggerated arousal.

In conclusion, we show that humans are capable of learning complex associations between the spatial location of objects within an environment and their aversive properties. Findings highlight a potential role for the anterior hippocampus, amygdala, and vmPFC in learning about the spatial context, the stimuli within it, and their associated value as flowers are approached. Recruitment of the dACC and insula when approaching danger suggests a role in cognitive and visceral appraisal of threat, with increased insula-hippocampal functional connectivity possibly reflecting the role of spatial context in driving interoceptive feelings of threat. As threat becomes imminent, dACC and insula activity, with increased connectivity between them, might contribute to ongoing appraisal processes and initiation of defensive behaviors via PAG, along with increased activity in the posterior hippocampus over time in line with its established role in representations of location. Observed differences in activity along the long-axis of the hippocampus during approach and threat imminence are consistent with the spatial scale of the anteroventral gradients in the hippocampus appropriate to current behavior. These results, along with the engagement of other areas described above, open the road to the understanding of how multiple complex representations relying on distinct brain areas could support threat learning and related behavioral expression. These findings may be particularly informative for research on psychological disorders in which patients often show a dysfunction of the brain areas and processes outlined here.

Methods

Participants. Twenty-seven healthy volunteers, aged 20-30 years, were recruited from the University College London student population. Before taking part, all participants provided written informed consent and, after completion, were debriefed and reimbursed for their time. The study was approved by the UCL Research Ethics Committee. All participants were right-handed and free from neurological or psychological impairment. Three participants were excluded from analyses due to technical issues during scanning, and two further participants were omitted as they were unable to explain the shock contingencies between the locations at the end of the task

(see procedure below). We, therefore, analyzed data from the remaining 22 participants (13 males; mean age=24.33; SD=3.20).

Virtual environment. A circular virtual environment was produced using Unity software (Unity Technologies, USA). The environment comprised of a circular grassland with a perimeter boundary wall surrounded by distal cues (mountains, sun, and clouds) presented at infinity for orienting, and two landmarks (beehives) placed within the environment (see **Fig. 1A and B**). The environment was presented in a first-person perspective, and participants could explore using a button box to move forward, turn left or right, and respond.

Skin conductance. Skin conductance was measured as an index of anxiety via 8mm Ag/AgCl electrodes attached to the medial phalanges of the index and middle fingers of the participant's left hand. Data were acquired using a custom-built constant voltage coupler (2.5v) with output converted into an optical pulse frequency. The optical signal was then converted to voltage pulses and recorded throughout the experiment (Micro 1401/Spike 2, Cambridge Electronic Design, Cambridge, UK).

Procedure. During the task, participants were instructed to move around the environment and pick flowers that appeared one at a time in random locations. All flowers used throughout the task were the same in visual appearance. On contact with a flower, the participant was held stationary for a variable duration (2000-8000ms; stationary period). During this period, they were asked to make a rating on a 0-to-9 scale concerning their expected likelihood of receiving a shock (0 for no shock, 9 for definite shock). This rating was performed via button presses of a slider, using one button to decrease the rating and another button to increase it. There were 80 flowers in total, with 40 situated in each half of the environment. Half of the environment was associated with danger, with flowers picked in this zone reinforced with shock on 50% of trials (danger), while flowers picked in the other half were never paired with shock (safe). After the stationary period, participants were free to move, and the next flower appeared in the environment. Shocks were applied using a Digitimer DS7A electrical stimulator (Digitimer, Welwyn Garden City, UK) and were delivered to the left hand with intensity up to 20mA for 2ms duration through a silver chloride electrode. Shock intensity was individually adjusted for each participant before starting the experiment. Individual adjustment procedures delivered a series of shocks to each subject, starting at 1.2mA. Subjects were asked to rate the level of pain with each shock on a 1-10 scale. Shock intensity was increased until the level was annoying, but not painful.

Interleaved with these flower-search trials, participants also performed spatial memory trials within the same environment in the absence of shocks, with one spatial memory trial occurring after every four flower trials. On each spatial memory trial, participants were required to learn the location of one of 4 objects (wooden box, gas can, book, and clock), which appeared in distinct locations; two objects appeared in each half of the environment. For the first four spatial memory trials, the object appeared in its location, and participants were instructed to collect the object and memorize its location. After the initial four spatial memory trials, 16 memory trials were carried out (4 per object) during the experiment. During these trials, participants' memory for object locations was tested. A static image of the object was presented in the top left corner of the screen, and the participant was required to move it to the object's home location. Upon arriving at the presumed home location of the object, participants pressed a button to indicate their response. After responding, a feedback phase was presented in which the object appeared in its correct location, and the participant had to collect it, strengthening the object location memory for the next time the same object was presented (see **Fig. S1**).

At the end of the experiment, participants were asked to name the four objects and their locations used during the spatial memory task, as well as explain the contingencies of danger and safety during threat learning. Participants who were unable to provide the objects' name and position, or explain the contingencies (n=2), were excluded from the final analysis.

Behavioral analysis. Skin conductance response data processing and analysis were performed using MATLAB. Skin conductance data were down-sampled to 200 Hz and then synchronized to the task. Skin conductance was assessed during two periods of the threat learning task. First, mean skin conductance level (SCL) during each approach quantified tonic skin conductance levels as participants navigated towards the flower. SCL was quantified from the last three-quarters of the approach period from flower appearance until trial completion. Skin conductance level was calculated by measuring the mean skin conductance from the beginning of active approach until before the flower was picked for each trial. Second, skin conductance responses were analyzed during the stationary period to examine phasic changes in anticipation to the shock outcome. Skin conductance responses were calculated for every trial by subtracting the minimum skin conductance during the stationary period (baseline) from the maximum response (peak) before the stimulus onset. Any response difference under 0.03 micro-Siemens was scored as zero. SCR was log transformed (log [1+SCR]) to normalize the distribution and then range correction ([SCR-SCRmin]/[SCRmax-SCRmin]) was applied to control for individual variation in responding (86). The same correction was applied to the skin conductance levels. For analyses,

SCRs and SCL were averaged into four equal blocks across the duration of the experiment, with each block including ten trials per condition (safe and danger).

Expectancy ratings taken at the beginning of each stationary period were analyzed in a similar way to skin conductance. Each rating provided (0-9) was averaged across trials to create four equal blocks across safe and danger conditions (10 trials in each block).

Finally, performance on the spatial memory task was analyzed by assessing distance error on each test trial. This distance error was calculated by taking the distance in virtual meters between the participant's response location when replacing the object and its correct location within the environment. Distance error was taken from each trial and averaged into four blocks (1 trial from each object in each block). All results were analyzed using a General Linear Model (GLM) for repeated measures using 2x4 ANOVAs to look for changes between conditions (safe, danger) and block (1 to 4). Bonferroni-corrected posthoc comparisons were conducted, and an alpha level of 0.05 was used.

fMRI acquisition. Blood oxygen level-dependent T2*-weighted functional images were acquired on a 3T Trio system (Siemens, Germany) using echo-planar imaging (EPI) with a 32 channel head coil. Images were acquired obliquely at 45° with the following parameters: repetition time, 3,360ms; echo time, 30ms; slice thickness, 2mm; inter-slice gap, 1mm; in-plane resolution, 3 × 3mm; field of view, 64 × 72mm^2; 48 slices per volume. A field map using a double echo FLASH sequence was recorded for distortion correction of the acquired EPI (87). After the functional scans, a T1-weighted 3-D MDEFT structural image (1mm^3) was acquired to co-register and display the functional data.

fMRI analysis. Data processing and analysis were performed using SPM8 (http://www.fil.ion.ucl.ac.uk/spm). EPI images were first preprocessed using a bias correction to control for within volume signal intensity difference, unwarping and realignment to correct for movement and slice-time correction. Images were then spatially normalized to the MNI template using parameter estimates from warping each participant's structural image to a T1-weighted average template image. All images were finally smoothed using an 8mm FWHM Gaussian kernel.

Statistical analyses occurred in two stages. The first-level model included 15 regressors of interest. Four separate regressors were created for approach periods, starting from the end of the

first quarter of each approach period to the point in which that flower was reached. Using a boxcar function, the regressors consisted of a 2x2 design (zone x block), divided by zone (safe or danger) and by block (first-half or last-half). A further four regressors were created for the stationary period of each trial, starting after the participant had rated their shock expectancy for the duration of the stationary period. These regressors were separated in the same way as approach periods (4 regressors). The end of each trial was also modeled using a stick function to account for whether participants received a shock, or not, across danger and safe conditions (3 regressors). Finally, trials when participants were approaching an object, and learning its location in the spatial memory task were modelled by using a boxcar function for the approach period to the location where the object had to be picked (4 regressors, first and second half of the experiment). Six regressors of no interest were also added to the model representing movement parameters estimated during realignment. Parameter estimates for conditions of interest were then entered into second level GLMs.

All analyses report family-wise error ($p<0.05$ FWE) corrected effects across the whole brain. Given the a priori hypotheses, effects in the bilateral hippocampus, amygdala, and mPFC that survive small volume correction (SVC; $p<0.05$ FWE) were reported. One bilateral mask comprising the hippocampus and a second bilateral mask for the mPFC that included the orbitofrontal gyrus, medial frontal gyrus, and anterior cingulate and medial cingulate gyrus was created, defined using the Automated Anatomical Labeling atlas (88), and implemented using the WFU Pickatlas toolbox in SPM8 (89). In accordance with previous studies, anterior and posterior regions of the hippocampus were identified relative to the first coronal slice in which the uncal apex was visible (90, 91).

To examine approach periods during threat learning, a second-level model was created to contrast approach to flowers associated with safety or danger and whether they were collected during the first or second half of the experiment. Therefore, approach periods were analyzed using a 2x2 ANOVA (zone, block). Periods when the flower was picked, and participants were held stationary, were analyzed in a similar second level model using a 2x2 ANOVA (zone, block). Finally, approach periods during threat learning (approaching flowers) was compared with approach periods during the spatial memory task (approaching location to replace the object). A second-level model was created contrasting approach periods for threat learning (collapsing across safety and danger) with approach during spatial memory across the first and second half of the experiment using a 2x2 ANOVA (task, block).

For any significant interaction, the representative time-course was extracted through SPM8 MarsBaR (http://marsbar.sourceforge.net) toolbox, using a 6mm sphere at the peak of the activity in the regions of interest, using the first eigenvariate calculated from singular value decomposition. The extracted values were analyzed in SPSS 22 on a 2x2 ANOVA (task x block) and further analyzed through a sample t-test, which was Bonferroni corrected.

Expectancy ratings and SCR were used as parametric modulation of interest to assess the correlation between BOLD signal (during active approach and stationary periods) and behavioral measures. However, as activity was not significantly modulated by SCR or expectancy ratings, we omit these analyses from the manuscript (whole brain parametric modulation analyses, $p>0.005$ uncorrected).

Functional connectivity analyses. Functional connectivity was assessed at group level using psychophysiological interactions (PPI) analysis using the SPM8 generalized psychophysiological interaction toolbox (92). The gPPI toolbox compares functional connectivity to a single seed region across tasks while accommodating for multiple task conditions in the same PPI model. The seed regions were selected based on a priori hypothesis of the connectivity of the vmPFC, dACC, PAG, and hippocampus to other areas during the task. Peak activation from these areas in the group level analysis, for approach and stationary periods, were used to create volumes of interest for each subject. The seed time series activity was extracted using a 6mm sphere at the center of the activation peak. Each seed region was assessed for task connectivity during active approach and stationary period. The individual t-contrast images of the interaction from the gPPI were examined using a group level one-sample t-test. The group PPI were detected using t-test with a threshold of $p<0.001$ uncorrected.

Acknowledgments

This work was supported by a Wellcome Trust Fellowship (202805/Z/16/Z) and European Research Council grant (ERC-2015-AdG, 694779) awarded to Neil Burgess. The authors are grateful to the Wellcome Trust Centre for Neuroimaging at UCL for providing facilities. We thank the National Institute of Mental Health and UCL Graduate Partnership Program and T32 grant MH015144 for providing support to B.S.J.

Author Contributions

BSJ, JAK, DSP, and NB designed the experiment.; BSJ programmed the VR task.; BSJ collected the data with contributions from JAB and AJH; BSJ and JAB analyzed the data with contributions from AJH and NB; BSJ, JAB, and NB interpreted the data.; BSJ, JAB, and NB wrote the manuscript with contributions from AJH, JAK, and DSP.

Competing Financial Interest

The authors declare no competing financial interests.

Data availability. The data presented in this article will be made available and referenced in publication.

Reference

1. Garfinkel SN et al. (2014) Impaired contextual modulation of memories in PTSD: an fMRI and psychophysiological study of extinction retention and fear renewal. *Journal of Neuroscience* 34:13435–13443.

2. Britton JC, Lissek S, Grillon C, Norcross MA, Pine DS (2011) Development of anxiety: the role of threat appraisal and fear learning. *Depress Anxiety* 28:5–17.

3. Kheirbek MA, Klemenhagen KC, Sahay A, Hen R (2012) Neurogenesis and generalization: a new approach to stratify and treat anxiety disorders. *Nat Neurosci* 15:1613–20.

4. Blanchard DC, Blanchard RJ (2008) Defensive behaviors, fear, and anxiety. *Handbook of behavioral neuroscience* 17:63–79.

5. Davis M, Walker DL, Miles L, Grillon C (2010) Phasic vs sustained fear in rats and humans: role of the extended amygdala in fear vs anxiety. *Neuropsychopharmacology: official publication of the American College of Neuropsychopharmacology* 35:105–135.

6. Sylvers P, Lilienfeld SO, LaPrairie JL (2011) Differences between trait fear and trait anxiety: implications for psychopathology. *Clinical psychology review* 31:122–137.

7. Tovote P, Fadok JP, Lüthi A (2015) Neuronal circuits for fear and anxiety. *Nature Reviews Neuroscience* 16:317–331.

8. Phillips RG, LeDoux JE (1992) Differential contribution of amygdala and hippocampus to cued and contextual fear conditioning. *Behav Neurosci* 106:274–85.

9. Fanselow MS, Fendt M (1999) The neuroanatomical and neurochemical basis of conditioned fear. *Neuroscience and biobehavioral reviews* 23:743–60.

10. LeDoux JE (2000) Emotion circuits in the brain. *Annual review of neuroscience* 23:155–184.

11. Blanchard DC, Blanchard RJ, Takahashi LK, Takahashi T (1977) Septal lesions and aggressive behavior. *Behavioral Biology* 21:157–161.

12. Maren S, Fanselow MS (1997) Electrolytic lesions of the fimbria/fornix, dorsal hippocampus, or entorhinal cortex produce anterograde deficits in contextual fear conditioning in rats. *Neurobiology of learning and memory* 67:142–149.

13. Kim JJ, Fanselow MS (1992) Modality-specific retrograde amnesia of fear. *Science* 256:675–7.

14. Burgess N, Maguire EA, O'Keefe J (2002) The human hippocampus and spatial and episodic memory. *Neuron* 35:625–641.

15. Morris R, Garrud P, Rawlins J, O'Keefe J (1982) Place navigation impaired in rats with hippocampal lesions. *Nature* 297:681–683.

16. O'keefe J, Nadel L (1978) *The hippocampus as a cognitive map* (Oxford: Clarendon Press).

17. Alvarez RP, Biggs A, Chen G, Pine DS, Grillon C (2008) Contextual fear conditioning in humans: cortical-hippocampal and amygdala contributions. *J Neurosci* 28:6211–9.

18. Kalisch R et al. (2006) Context-dependent human extinction memory is mediated by a ventromedial prefrontal and hippocampal network. *J Neurosci* 26:9503–11.

19. Bannerman DM et al. (2014) Hippocampal synaptic plasticity, spatial memory and anxiety. *Nat Rev Neurosci* 15:181–92.

20. Bannerman D et al. (1999) Double dissociation of function within the hippocampus: a comparison of dorsal, ventral, and complete hippocampal cytotoxic lesions. *Behavioral neuroscience* 113:1170.

21. Fanselow MS, Dong H-W (2010) Are the dorsal and ventral hippocampus functionally distinct structures? *Neuron* 65:7–19.

22. Kheirbek MA et al. (2013) Differential control of learning and anxiety along the dorsoventral axis of the dentate gyrus. *Neuron* 77:955–68.

23. Kjelstrup KG et al. (2002) Reduced fear expression after lesions of the ventral hippocampus. *Proc Natl Acad Sci USA* 99:10825–30.

24. Moser MB, Moser EI (1998) Functional differentiation in the hippocampus. *Hippocampus* 8:608–19.

25. Aggleton JP (2012) Multiple anatomical systems embedded within the primate medial temporal lobe: implications for hippocampal function. *Neurosci Biobehav Rev* 36:1579–96.

26. Strange BA, Witter MP, Lein ES, Moser EI (2014) Functional organization of the hippocampal longitudinal axis. *Nat Rev Neurosci* 15:655–69.

27. Poppenk J, Evensmoen HR, Moscovitch M, Nadel L (2013) Long-axis specialization of the human hippocampus. *Trends Cogn Sci (Regul Ed)* 17:230–40.

28. Doeller CF, King JA, Burgess N (2008) Parallel striatal and hippocampal systems for landmarks and boundaries in spatial memory. *Proc Natl Acad Sci USA* 105:5915–20.

29. Kaplan R, Horner AJ, Bandettini PA, Doeller CF, Burgess N (2014) Human hippocampal processing of environmental novelty during spatial navigation. *Hippocampus* 24:740–50.

30. Bach DR et al. (2014) Human hippocampus arbitrates approach-avoidance conflict. *Curr Biol* 24:541–7.

31. Etkin A, Egner T, Kalisch R (2011) Emotional processing in anterior cingulate and medial prefrontal cortex. *Trends Cogn Sci (Regul Ed)* 15:85–93.

32. Linnman C et al. (2012) Resting amygdala and medial prefrontal metabolism predicts functional activation of the fear extinction circuit. *Am J Psychiatry* 169:415–23.

33. Shin LM et al. (2009) Resting metabolic activity in the cingulate cortex and vulnerability to posttraumatic stress disorder. *Arch Gen Psychiatry* 66:1099–107.

34. Milad MR, Quirk GJ (2002) Neurons in medial prefrontal cortex signal memory for fear extinction. *Nature* 420:70–74.

35. Motzkin JC, Philippi CL, Wolf RC, Baskaya MK, Koenigs M (2014) Ventromedial Prefrontal Cortex Is Critical for the Regulation of Amygdala Activity in Humans. *Biological psychiatry*.

36. Phelps EA, Delgado MR, Nearing KI, LeDoux JE (2004) Extinction learning in humans: role of the amygdala and vmPFC. *Neuron* 43:897–905.

37. Schiller D, Levy I, Niv Y, LeDoux JE, Phelps EA (2008) From fear to safety and back: reversal of fear in the human brain. *J Neurosci* 28:11517–25.

38. Rauch SL, Shin LM, Phelps EA (2006) Neurocircuitry models of posttraumatic stress disorder and extinction: human neuroimaging research-past, present, and future. *Biol Psychiatry* 60:376–382.

39. Delgado MR et al. (2016) Viewpoints: dialogues on the functional role of the ventromedial prefrontal cortex. *Nature neuroscience* 19:1545–1552.

40. Adhikari A, Topiwala MA, Gordon JA (2010) Synchronized activity between the ventral hippocampus and the medial prefrontal cortex during anxiety. *Neuron* 65:257–69.

41. Adhikari A, Topiwala MA, Gordon JA (2011) Single units in the medial prefrontal cortex with anxiety-related firing patterns are preferentially influenced by ventral hippocampal activity. *Neuron* 71:898–910.

42. Clithero JA, Rangel A (2013) Informatic parcellation of the network involved in the computation of subjective value. *Social cognitive and affective neuroscience*:nst106.

43. Kennerley SW, Walton ME (2011) Decision making and reward in frontal cortex: complementary evidence from neurophysiological and neuropsychological studies. *Behav Neurosci* 125:297–317.

44. Rushworth MFS, Noonan MP, Boorman ED, Walton ME, Behrens TE (2011) Frontal cortex and reward-guided learning and decision-making. *Neuron* 70:1054–69.

45. Alexander WH, Brown JW (2011) Medial prefrontal cortex as an action-outcome predictor. *Nat Neurosci* 14:1338–44.

46. Euston DR, Gruber AJ, McNaughton BL (2012) The role of medial prefrontal cortex in memory and decision making. *Neuron* 76:1057–70.

47. Miller EK, Cohen JD (2001) An integrative theory of prefrontal cortex function. *Annu Rev Neurosci* 24:167–202.

48. Bouton ME, Mineka S, Barlow DH (2001) A modern learning theory perspective on the etiology of panic disorder. *Psychol Rev* 108:4–32.

49. Gray JA, McNaughton N (1996) The neuropsychology of anxiety: reprise. *Nebr Symp Motiv* 43:61–134.

50. Fanselow MS, Lester LS (1988) A functional behavioristic approach to aversively motivated behavior: Predatory imminence as a determinant of the topography of defensive behavior.

51. Fanselow MS (1994) Neural organization of the defensive behavior system responsible for fear. *Psychon Bull Rev* 1:429–38.

52. Amir A, Lee S-C, Headley DB, Herzallah MM, Pare D (2015) Amygdala signaling during foraging in a hazardous environment. *Journal of Neuroscience* 35:12994–13005.

53. Bechara A, Tranel D, Damasio H, Adolphs R, others (1995) Double dissociation of conditioning and declarative knowledge relative to the amygdala and hippocampus in humans. *Science* 269:1115.

54. Blanchard DC, Blanchard RJ (1972) Innate and conditioned reactions to threat in rats with amygdaloid lesions. *J Comp Physiol Psychol* 81:281–90.

55. Johansen JP, Tarpley JW, LeDoux JE, Blair HT (2010) Neural substrates for expectation-modulated fear learning in the amygdala and periaqueductal gray. *Nat Neurosci* 13:979–86.

56. Fanselow MS (1992) The midbrain periaqueductal gray as a coordinator of action in response to fear and anxiety. *The midbrain periaqueductal gray matter*:151–173.

57. Mobbs D et al. (2009) From threat to fear: the neural organization of defensive fear systems in humans. *J Neurosci* 29:12236–43.

58. Mobbs D et al. (2007) When fear is near: threat imminence elicits prefrontal-periaqueductal gray shifts in humans. *Science* 317:1079–83.

59. Friston KJ et al. (1997) Psychophysiological and Modulatory Interactions in Neuroimaging. *NeuroImage* 6:218–229.

60. LeDoux J (1996) Emotional networks and motor control: a fearful view. *Prog Brain Res* 107:437–46.

61. Sierra-Mercado D, Padilla-Coreano N, Quirk GJ (2011) Dissociable roles of prelimbic and infralimbic cortices, ventral hippocampus, and basolateral amygdala in the expression and extinction of conditioned fear. *Neuropsychopharmacology* 36:529–538.

62. Lin W-J, Horner AJ, Burgess N (2016) Ventromedial prefrontal cortex, adding value to autobiographical memories. *Sci Rep* 6:28630.

63. LaBar KS, Cabeza R (2006) Cognitive neuroscience of emotional memory. *Nature Reviews Neuroscience* 7:54–64.

64. Fletcher P et al. (1995) The mind's eye—precuneus activation in memory-related imagery. *Neuroimage* 2:195–200.

65. Katche C, Dorman G, Slipczuk L, Cammarota M, Medina JH (2013) Functional integrity of the retrosplenial cortex is essential for rapid consolidation and recall of fear memory. *Learning \& memory* 20:170–173.

66. Craig ADB (2009) Emotional moments across time: a possible neural basis for time perception in the anterior insula. *Philos Trans R Soc Lond, B, Biol Sci* 364:1933–42.

67. Critchley HD, Wiens S, Rotshtein P, Öhman A, Dolan RJ (2004) Neural systems supporting interoceptive awareness. *Nature neuroscience* 7:189–195.

68. Kober H et al. (2008) Functional grouping and cortical-subcortical interactions in emotion: a meta-analysis of neuroimaging studies. *Neuroimage* 42:998–1031.

69. Mechias M-L, Etkin A, Kalisch R (2010) A meta-analysis of instructed fear studies: implications for conscious appraisal of threat. *Neuroimage* 49:1760–8.

70. Kjelstrup KB et al. (2008) Finite scale of spatial representation in the hippocampus. *Science* 321:140–143.

71. Collin SHP, Milivojevic B, Doeller CF (2015) Memory hierarchies map onto the hippocampal long axis in humans. *Nat Neurosci* 18:1562–4.

72. Deakin JW, Graeff FG (1991) 5-HT and mechanisms of defence. *Journal of psychopharmacology* 5:305–315.

73. McNaughton BL (1993) The mechanism of expression of long-term enhancement of hippocampal synapses: current issues and theoretical implications. *Annu Rev Physiol* 55:375–96.

74. Vianna DM, Graeff FG, Brandão ML, Landeira-Fernandez J (2001) Defensive freezing evoked by electrical stimulation of the periaqueductal gray: comparison between dorsolateral and ventrolateral regions. *Neuroreport* 12:4109–4112.

75. Devinsky O, Morrell MJ, Vogt BA (1995) Contributions of anterior cingulate cortex to behaviour. *Brain* 118:279–306.

76. Depaulis A, Bandler R, Vergnes M (1989) Characterization of pretentorial periaqueductal gray matter neurons mediating intraspecific defensive behaviors in the rat by microinjections of kainic acid. *Brain Research* 486:121–132.

77. De la Vega A, Chang LJ, Banich MT, Wager TD, Yarkoni T (2016) Large-scale meta-analysis of human medial frontal cortex reveals tripartite functional organization. *Journal of Neuroscience* 36:6553–6562.

78. Zhang Z, Mendelsohn A, Manson KF, Schiller D, Levy I (2015) Dissociating value representation and inhibition of inappropriate affective response during reversal learning in the ventromedial prefrontal cortex. *eNeuro* 2:ENEURO–0072.

79. Paulus MP, Stein MB (2006) An insular view of anxiety. *Biol Psychiatry* 60:383–7.

80. Etkin A, Wager TD (2007) Functional neuroimaging of anxiety: a meta-analysis of emotional processing in PTSD, social anxiety disorder, and specific phobia. *American Journal of Psychiatry* 164:1476–1488.

81. Milad MR et al. (2009) Neurobiological basis of failure to recall extinction memory in posttraumatic stress disorder. *Biol Psychiatry* 66:1075–82.

82. Kaplan R et al. (2012) Movement-related theta rhythm in humans: coordinating self-directed hippocampal learning. *PLoS biology* 10:e1001267.

83. Kaplan R et al. (2014) Medial prefrontal theta phase coupling during spatial memory retrieval. *Hippocampus* 24:656–665.

84. Mueller SC et al. (2009) Impaired spatial navigation in pediatric anxiety. *J Child Psychol Psychiatry* 50:1227–34.

85. Cornwell BR, Overstreet C, Krimsky M, Grillon C (2013) Passive avoidance is linked to impaired fear extinction in humans. *Learn Mem* 20:164–9.

86. Lykken D (1972) Range correction applied to heart rate and to GSR data. *Psychophysiology* 9:373–379.

87. Weiskopf N, Hutton C, Josephs O, Deichmann R (2006) Optimal EPI parameters for reduction of susceptibility-induced BOLD sensitivity losses: a whole-brain analysis at 3 T and 1.5 T. *Neuroimage* 33:493–504.

88. Tzourio-Mazoyer N et al. (2002) Automated anatomical labeling of activations in SPM using a macroscopic anatomical parcellation of the MNI MRI single-subject brain. *Neuroimage* 15:273–289.

89. Maldjian JA, Laurienti PJ, Kraft RA, Burdette JH (2003) An automated method for neuroanatomic and cytoarchitectonic atlas-based interrogation of fMRI data sets. *Neuroimage* 19:1233–9.

90. Weiss AP, Dewitt I, Goff D, Ditman T, Heckers S (2005) Anterior and posterior hippocampal volumes in schizophrenia. *Schizophrenia research* 73:103–12.

91. Poppenk J, Moscovitch M (2011) A hippocampal marker of recollection memory ability among healthy young adults: contributions of posterior and anterior segments. *Neuron* 72:931–7.

92. McLaren DG, Ries ML, Xu G, Johnson SC (2012) A generalized form of context-dependent psychophysiological interactions (gPPI): a comparison to standard approaches. *Neuroimage* 61:1277–86.

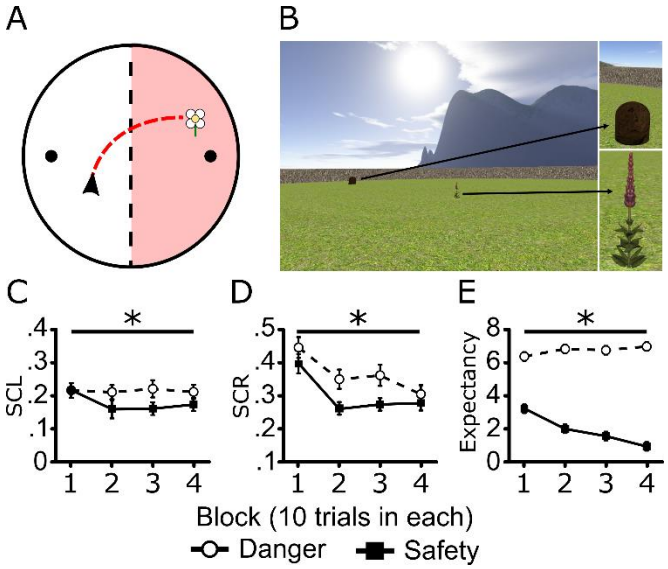

Figure 1. Task illustration and behavioral data across threat learning. (A) Overhead illustration of the circular environment that participants explored and how it was split into one-half associated with danger (red) and the other with safety. The environment included two beehives (black dots) located at opposite sides of the environment. Participants were required to collect flowers, which were generated within the environment. (B) Example of the participant's viewpoint, showing a beehive and flower within the environment. (C) Mean tonic skin conductance level (SCL) as flowers were approached. (D) Mean phasic skin conductance responses (SCR) during the stationary periods when flowers were picked. (E) Shock expectancy ratings at the onset of stationary periods when picking a flower. Error bars show SEM, *p<0.01.

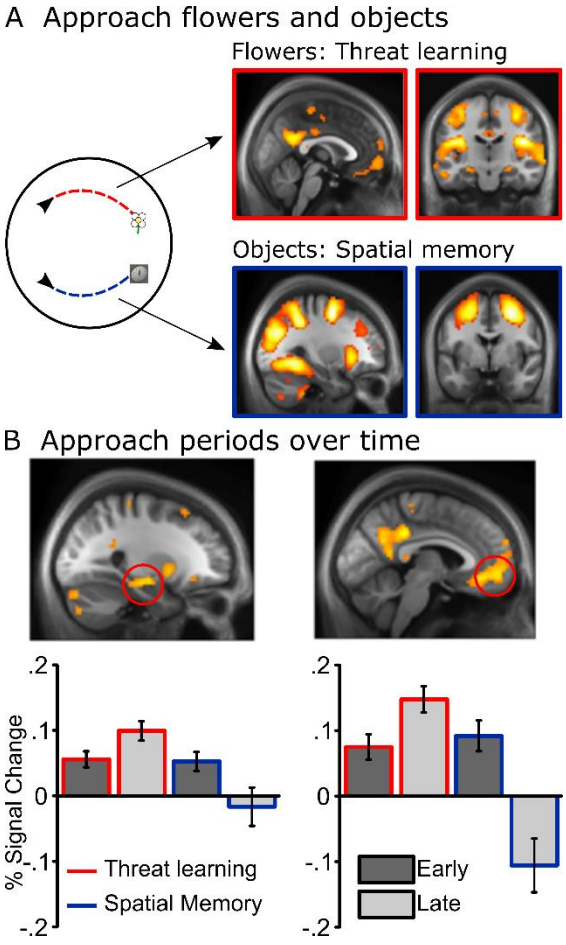

Figure 2. Activity differences between approaching flowers and objects during threat and spatial memory, respectively. (A upper red panel) Greater activity when approaching flowers compared to objects in a range of areas, including the insula, medial parietal cortex, PCC ($p<.0.05$ FWE), vmPFC, bilateral anterior hippocampus, and amygdala ($p<0.05$ FWE SVC). (A lower blue panel) When approaching objects compared to flowers, greater activity was seen in posterior medial temporal, parietal, and prefrontal neocortical areas ($p<0.05$ FWE). (B) Activity change was greater from the first to the second half of the flower task compared to activity change during the object location task in anterior hippocampus and amygdala ($p<0.05$ FWE SVC; left panel) and vmPFC, medial parietal cortices/precuneus, and PCC ($p<0.05$ FWE; right panel). All images are presented at $p<0.001$ uncorrected for display purposes. Percentage signal changes for learning about threat and object locations across early and late periods of the task extracted from anterior hippocampus (MNI coordinates: 27, -18, -15; B left panel) and vmPFC (3, 54, -9; B right panel). Error bars show SEM.

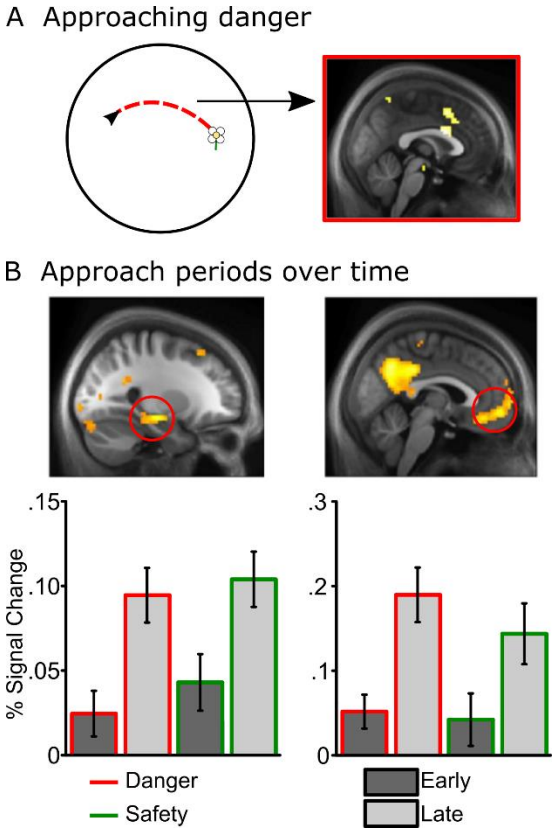

Figure 3. Activity differences when approaching flowers across danger and safety. (A) For flowers approached in the danger compared to the safe zone, there was greater activity in dACC across the whole test session. (B) Irrespective of the location of flowers, activity increased from the first to second half of the experiment in the anterior hippocampus (left panel) and vmPFC and medial parietal areas (including precuneus, retrosplenial cortex, and PCC; right panel). All images are presented at $p<0.001$ uncorrected for display purposes. Percentage signal changes for danger and safety across early and late periods of learning extracted from anterior hippocampus (MNI coordinates: 27, -18, -15; B left panel) and vmPFC (3, 54, -9; B right panel). Error bars show SEM.

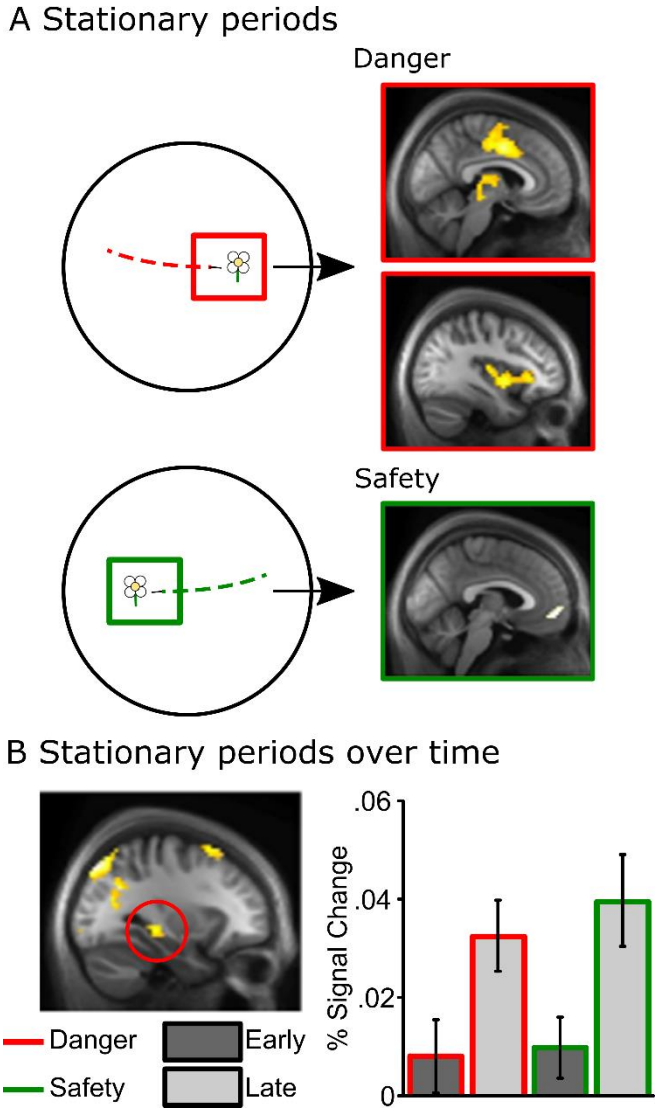

Figure 4. Activity differences during stationary periods after picking flowers predicting danger and safety. (A) Contrasting periods when participants were stationary when flowers were picked in the dangerous versus safe zone of the environment showed greater activity in periaqueductal gray, dACC (upper panel), and bilateral insula ($p<0.05$ FWE; middle panel). Analysis of the reverse contrast for flowers picked in the safe zone (safe > danger) showed greater activity in the vmPFC ($p<0.001$ uncorrected; lower panel). (B) Irrespective of the location of flowers, during the last half of learning (late > early), we saw greater activity in bilateral posterior hippocampus ($p<0.05$ FWE SVC). Images are presented at $p<0.001$ uncorrected for display purposes. (B right) Percentage signal change during stationary periods for danger and safety across early and late parts of learning extracted posterior hippocampus (MNI coordinates: 33, -33, -3). Error bars show SEM.

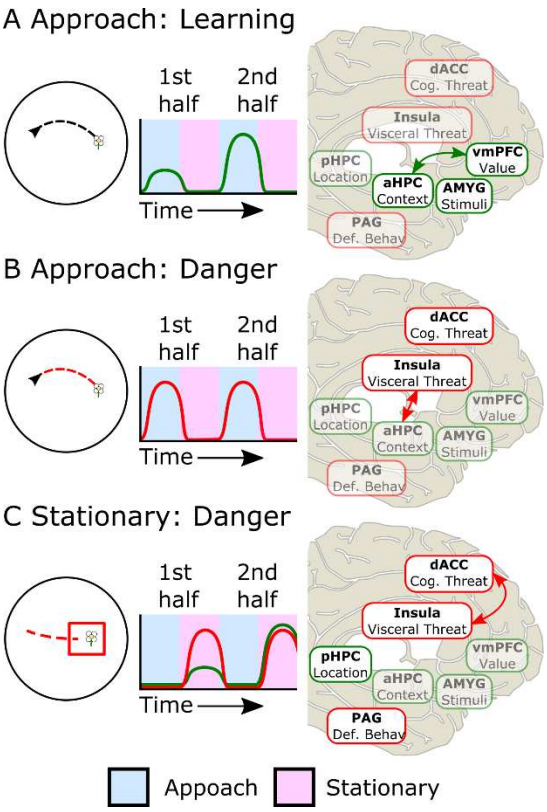

Figure 5. Illustration of sequential network activity in the flower task. (A) During approach periods, activity in the anterior hippocampus (aHPC), amygdala (AMYG) and ventromedial prefrontal cortex (vmPFC) increased in the late compared to the early-phase of learning, including greater functional connectivity between aHPC and vmPFC, irrespective of threat. (B) Approach to flowers predicting danger was associated with increased activity in the dorsal anterior cingulate cortex (dACC), and insula, with increased connectivity, also observed between dACC and aHPC. (C) When danger was imminent, during the stationary period, increased activity was evident in dACC, insula (as well as connectivity between them) and periaqueductal grey (PAG). The posterior hippocampus (pHPC) also showed greater activity during the last-half of the experiment when picking the flower compared to the first half. **Left:** illustration of task phase. **Middle:** schematic of activity over time (first- and second-half of experiment; approach periods in blue, stationary periods in pink). **Right:** Brain activity and functional connectivity. Green lines and boxes represent activity (and green arrows functional connectivity) that increases from the first to second half of the experiment. Red lines and boxes represent activity (and red arrows functional connectivity) that increases with danger. See Tables S1-3 for a complete breakdown of regions across these analyses.

Supplementary Results

Performance on the spatial memory task was analyzed by assessing distance error on each test trial. This error was calculated by taking the distance in virtual meters between the participant's response location when replacing the object and its correct location within the environment. Distance error was taken from each trial and averaged into four blocks (1 trial from each object in each block; 4 trials per block). All results were analyzed using a General Linear Model (GLM) for repeated measures using 2x4 ANOVAs to look for changes between conditions (safe, danger) and block (1 to 4). Bonferroni-corrected posthoc comparisons were conducted, and an alpha level of 0.05 was used.

A 2x4 within-subjects ANOVA (zone x block) measuring error rate of object placement showed a significant effect of block ($F(3,63)=14.98$, $p<0.01$), showing error decreased over time regardless of the zone. There was no significant effect of zone ($F(1,21)=0.94$, $p>0.05$) or interaction between zone x block ($F(3,63)=0.96$, $p>0.05$) (**Fig. S1**).

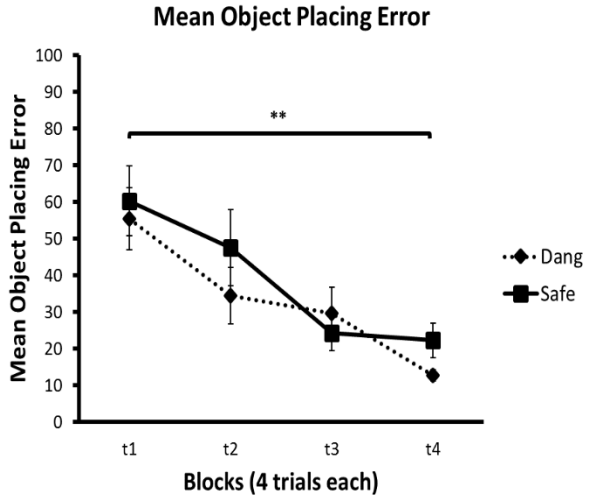

Fig. S1. Experiment 4 Mean object placement error. *Mean object placement error, for the safe zone (Safe) and the dangerous zone (Dang) over time. Error bars show SEM, **p<0.01.*

Table S1. Summary of imaging findings when approaching flowers during threat learning or objects during spatial memory encoding.

Region	Laterality	MNI coordinates x	y	z	z-score
Task (flower, object) x block (early, late)					
Main effect of approaching flowers (flower > object)					
Insula / Rolandic operculum	L	45	-18	21	7.26
	R	-54	-6	9	6.61
Middle temporal gyrus	R	-45	3	-30	6.02
Postcentral gyrus	R	30	-27	60	6.00
	L	-48	-18	48	4.66
Precentral gyrus	R	33	-21	54	5.76
Inferior occipital gyrus	L	-21	-99	-6	5.44
Posterior cingulate cortex	R	3	-51	27	5.42
Cerebellum	R	30	-84	-30	5.05
Putamen	L	-27	-6	-3	4.95
Dorsomedial prefrontal cortex†	R	9	-30	63	4.90
Ventromedial prefrontal cortex†	L	-9	54	39	4.59
Hippocampus†	R	27	-15	-15	3.97
	L	-30	-15	-15	3.78
Amygdala†	R	27	-9	-15	3.97
	L	-21	-9	-12	3.81
Main effect of approaching objects (object > flower)					
Precentral gyrus	R	30	-3	51	>8.00
Middle frontal gyrus	L	-30	-51	-9	>8.00
Lingual gyrus	R	24	-60	-6	>8.00
Cerebellum	L	-12	-54	-48	7.60
	R	12	-51	-51	7.01
Middle temporal gyrus	L	-54	-60	-3	6.26
Inferior parietal lobe	L	-57	-33	39	6.05
Insula	L	-36	21	0	5.59
Inferior temporal gyrus	R	57	-54	-3	5.42
Inferior frontal gyrus	R	-36	-72	-45	4.90
Task (flower > object) x block (late > early) interaction					
Ventromedial prefrontal cortex	R	3	54	-9	5.63
Hippocampus†	R	27	-18	-15	4.34
	L	-30	-15	-15	3.39
Amygdala†	R	27	-9	-15	3.93
	L	-21	-9	-15	3.78

$p<0.05$ FWE across whole brain unless stated; $^{\dagger}p<0.05$ FWE SVC

Table S2. Summary of imaging findings when approaching flowers predicting danger or safety.

Region	Laterality	MNI coordinates x	y	z	z-score
Threat (danger, safety) x block (early, late)					
Main effect of threat (danger > safe)					
Dorsal anterior cingulate†		0	9	27	4.24
Insula*	L	-36	21	3	3.82
	R	39	27	3	3.69
Main effect of block (late > early)					
Angular gyrus	L	-45	-72	30	6.04
Posterior medial cingulate cortex	L	-3	-39	36	5.53
Middle frontal gyrus	L	-24	24	51	5.27
Precuneus	R	6	-57	39	5.21
Posterior cingulate cortex	R	9	-48	15	4.76
Hippocampus	R	27	-18	-15	4.75
	L	-21	-21	-18	4.49
Ventromedial prefrontal cortex	R	3	54	-9	4.68
Main effect of block (early > late)					
Inferior frontal gyrus	R	51	12	15	5.29
Postcentral gyrus	R	63	-18	33	5.08
Supramarginal gyrus	L	-63	-24	30	4.88
	R	33	27	3	4.80
Insula	R	57	-36	36	4.79

$p<0.05$ FWE across whole brain unless stated; $^{\dagger}p<0.05$ FWE SVC; *$p<0.001$uncorrected

Table S3. Summary of imaging findings during freezing periods for flowers during danger and safety.

Region	Laterality	MNI coordinates x	y	z	z-score
Threat (danger, safety) x block (early, late)					
Main effect of threat (danger > safety)					
Supramarginal gyrus	L	-66	-24	21	7.38
	R	54	-21	24	7.10
Doral anterior cingulate cortex	R	6	0	39	6.66
Postcentral gyrus	R	21	-42	63	6.53
Insula	L	-36	0	-3	6.24
	R	35	3	-5	5.77
Thalamus	R	12	-18	9	6.02
Periaqueductal grey	R	6	-24	3	5.11
Posterior medial cingulate cortex	L	-12	-27	39	5.04
Middle temporal gyrus	L	-51	-63	9	4.98
Superior frontal gyrus	R	18	-12	72	4.79
Cerebellum	L	-21	-57	-51	4.77
Dorsomedial prefrontal cortex	L	-6	-9	66	4.75
Main effect of threat (safety > danger)					
Ventromedial prefrontal cortex*	L	-3	48	-9	3.59
Task (flower > object) x block (late > early) interaction					
Inferior parietal lobule	L	-30	-78	48	5.37
Angular gyrus	L	-45	-72	42	4.84
Hippocampus†	R	33	-33	-3	4.25
	L	-30	-33	-6	4.22

*$p<0.05$ FWE across whole brain unless stated; †$p<0.05$ FWE SVC